Journal of Catalysis 279 (2011) 136–143

Contents lists available at ScienceDirect

Journal of Catalysis

journal homepage: www.elsevier.com/locate/jcat

Mechanism of acetic acid esterification over sulfonic acid-functionalized mesoporous silica

Shaojun Miao, Brent H. Shanks *

Department of Chemical and Biological Engineering, Iowa State University, Ames, IA 50011, USA

ARTICLE INFO

Article history:
Received 25 August 2010
Revised 15 December 2010
Accepted 10 January 2011
Available online 12 February 2011

Keywords:
Acid-functionalized mesoporous silicas
Organic–inorganic hybrid catalysts
Acetic acid esterification
Esterification reaction mechanism

ABSTRACT

The kinetics of acetic acid esterification with methanol using a propylsulfonic acid-functionalized SBA-15 catalyst were investigated. To determine whether a different mechanism was applicable for heterogeneous or homogeneous catalyzed esterification, propane sulfonic acid was also examined as this homogeneous acid has the same structure as the functional groups tethered onto SBA-15. In isothermal experiments at 323 K, the apparent reaction orders using the heterogeneous catalyst were determined to be 0.72 for methanol and 0.87 for acetic acid. Reactant adsorption studies showed that pre-adsorption of acetic acid hindered the reaction rate, while pre-adsorption of methanol or acetic acid with methanol increased the reaction rate, indicating that acetic acid adsorbs more strongly than methanol over the heterogeneous acid catalyst. The experimental results demonstrated that acetic acid esterification with methanol followed a dual-site Langmuir–Hinshelwood type reaction mechanism, which required both the adsorption of acetic acid and methanol over propylsulfonic acid-functionalized SBA-15. In contrast, esterification reaction with the homogeneous catalyst followed an Eley–Rideal mechanism. The kinetic data were successfully fit with a model in which the surface reaction was the rate-limiting step.

1. Introduction

Esters of carboxylic acids are important in a variety of products, ranging from perfumes to biofuels. The latter is of particular significance due to the rising price of crude oil and environmental concerns. Several synthetic routes are available for producing organic esters, most of which have been briefly reviewed by Yadav and Mehta [1]. The most-used methodology for ester synthesis is the direct esterification of carboxylic acids with alcohols, which is conventionally conducted in the liquid phase, using batch reactors and strong liquid mineral acids, such as H_2SO_4, HCl, and HI, as the catalyst. However, this processing approach requires additional catalyst neutralization and separation steps with the catalyst being disposed as salts, which generally increases processing costs. Alternatively, solid catalysts can be easily separated from reaction products and can be, in most cases, used for multiple reaction cycles. In addition, solid catalysts can be more easily used in continuous processing operations, further improving the economics of ester manufacture. For these reasons, there is significant interest in developing solid acid catalysts for esterification applications.

The kinetic model and reaction mechanism for carboxylic acids esterification over homogeneous acids have been well documented in which a protonated carboxylic acid is attacked by a nucleophilic alcohol molecule, yielding an ester and water [2]. Using solid acid catalysts containing primarily Brønsted acid sites, one might expect to have similar esterification behavior with an analogous mechanism to that in the homogeneous system mediating the molecular transformation [3]. However, results in the literature concerning the fundamental aspects of solid acid-catalyzed esterification reactions are ambiguous at best. Mainly, two mechanisms for esterification on heterogeneous acid catalysts have been proposed: a single-site mechanism (Eley–Rideal type, E–R) [4–8] and a dual-site mechanism (Langmuir–Hinshelwood type, L–H) [3,9,10]. Esterification work done in the Goodwin group demonstrated that the esterification of acetic acid with short-chain alcohols (methanol and ethanol) over silica-supported Nafion (SAC-13), which contained only Brønsted acid sites, proceeded via a single-site mechanism, whether in the gas phase for the temperature range of 90–140 °C [6] or in the condensed phase for temperatures of $\leqslant$60 °C [4] primarily based on results from pyridine poisoning experiments. Also, an E–R kinetic model was found to yield better results with 15% less error in fitting the experimental reaction results for the esterification of hexanoic acid with 1-octanol using zeolite BEA and SAC-13 [7]. In contrast, Teo and Saha [9] and Lee et al. [10] found that a dual-site model better fit the behavior of acid resin catalysts used in the esterification of acetic acid with amyl alcohol using kinetic correlations of experimental data. Using transient and steady-state experiments, isotopic labeling experiments and temperature-programmed desorption (TPD), Koster

* Corresponding author. Fax: +1 515 294 2689.
E-mail address: bshanks@iastate.edu (B.H. Shanks).

0021-9517/$ - see front matter © 2011 Elsevier Inc. All rights reserved.
doi:10.1016/j.jcat.2011.01.008

et al. [3] suggested that the gas-phase reaction of acetic acid with ethanol on MCM-41 was performed through a dual-site mechanism in which both acetic acid and ethanol must be adsorbed on the surface for the reaction to occur. However, Chu et al. [11] reported that alcohol structure had a profound effect on the mechanism of the gas-phase esterification of acetic acid changing from a dual-site mechanism for ethanol to a single-site mechanism for *n*-butanol.

In this study, a heterogeneous acid catalyst, propylsulfonic acid-functionalized mesoporous silica, was prepared by a co-condensation method and employed as the catalyst for the kinetics study of esterification of acetic acid. This reaction system has potentially important application in the upgrading of fast pyrolysis-derived bio-oil for fuel applications [12,13]. Mesoporous silica materials–supported organic acid is an attractive heterogeneous acid catalyst due to its high surface area, good control of the acid moieties, no significant Lewis acidic sites and good stability without swelling in organic solvents. The focus of the present study was to provide fundamental insight into the similarities and differences existing between heterogeneous and homogeneous Brønsted acid catalysts in the esterification reaction. Propane sulfonic acid was chosen as the homogeneous acid catalyst for comparison since it bears the same structure as the grafted functional groups in the above heterogeneous catalyst.

2. Experimental

2.1. Chemicals and synthesis

SBA-15-functionalized organosulfonic acid materials were synthesized by one-pot co-condensation method as described previously [14–16]. Tetraethoxysilane (TEOS) (98%, Aldrich) was used as the silica precursor, and (3-mercaptopropyl)trimethoxysilane (MPTMS) (85%, Acros) was used without further purification as the organosulfonic acid source. Pluronic P123 (BASF Co., USA), which is a tri-block copolymer of polyethylene oxide–polypropylene oxide–polyethylene oxide, was used as obtained to tailor the textural properties of the mesoporous materials. In a typical one-step synthesis, 4 g of Pluronic P123 was dissolved in 125 g of 1.9 M HCl at room temperature with continuous stirring. The solution was subsequently heated to 313 K before adding TEOS. As usual, TEOS was pre-hydrolyzed for approximately 45 min prior to the addition of the MPTMS-H_2O_2 solution. The molar composition of the resulting mixture was 0.0369 TEOS, 0.0062 MPTMS, and 0.0554 H_2O_2. It was continuously stirred for 24 h at 313 K and thereafter aged for 24 h at 373 K under static conditions. The product was collected and subjected to ethanol refluxing for three cycles for the extraction of the template. The final product was vacuum dried at 373 K for 6 h.

2.2. Sample characterization

Nitrogen adsorption–desorption isotherms were measured at liquid nitrogen temperature with a Micromeritics ASAP 2020 system. Prior to measurement, all samples were degassed at 373 K for 6 h. The specific surface areas were evaluated using the Brunauer–Emmett–Teller (BET) method and pore size distribution curves were calculated using the desorption branch of the isotherms and the Barrett–Joyner–Halenda (BJH) method. The content of organic material present in the solids was determined by elemental analysis performed on a Perkin-Elmer Series II 2400 CHNS analyzer. The decomposition temperature of the organic composition in the modified mesoporous materials was determined by thermogravimetric analysis (TGA) with a Perkin-Elmer TGA7 instrument, with heating from 323 to 973 K at a ramp of 10 K/min under flowing air. The ion capacities of the sulfonic acid groups in the functionalized mesoporous silica were quantified using 2 M NaCl (aq) as the ion-exchange agent. Approximately 0.05 g of the sample was added to 30 ml of the salt solution and allowed to equilibrate for 18 h. Thereafter, it was titrated by dropwise addition of 0.005 M NaOH (aq) [15].

2.3. Catalytic reactions

The kinetic measurement of esterification of acetic acid with methanol was carried out in a stirred batch reactor, which was placed in a thermostatic bath with a magnetic stirrer. The temperature in the reactor was maintained within ±0.2 K. The reactor was charged with a measured amount of reagents (acetic acid 3 M, methanol 6 M, as well as the solvent 1,4-dioxane to balance the total volume to 50 ml). When the mixture was heated to the desired reaction temperature, the first sample was taken as the zero point for every run, after which an exact amount of catalyst was added to initiate the reaction. In all cases, a microscale syringe was used for sampling at definite time intervals. Stirring speed of 600 rpm was applied to rule out mass transfer limitation as previously reported [12]. Kinetic measurement was performed at low acetic acid conversion (<10%). Pyridine adsorption experiments were carried out by immersing a known amount of catalyst in 1,4-dioxane containing a known amount of pyridine overnight. The reaction started by heating the above mixture to the desired temperature and charging the preheated acetic acid and methanol. The pre-adsorption experiments were performed by premixing the catalyst with one of the reactants or both and solvent at ambient temperature overnight followed by heating to the desired temperature and charging the preheated other one. For the pre-adsorption of catalyst with both acetic acid and methanol, small amounts of acetic acid and methanol (0.5 g acetic acid and 0.5 g methanol) were used with 1,4-dioxane to premix with catalyst overnight and the remaining were charged to start the reaction. An Agilent GC 7890A gas chromatograph equipped with a HP-5 column (0.32 mm × 30 m × 0.25 μm) and a FID detector was used for sample analysis. The concentrations of all species except water were directly quantified. The overall mass balance was more than 98%.

2.4. Computational method

Computational modeling was used to examine whether the adsorption behavior observed experimentally was consistent with molecular energetic. A simple representation of the catalyst surface was used in which the central Si atom was bound to the tethered organosulfonic acid and three O atoms, which were also bonded to a second Si atom. These terminal Si atoms were saturated with hydrogen atoms at a Si–H distance of 1.46 Å in the calculations. The $(SiH_4)_3$ groups were held fixed, while the other atoms were allowed to relax during the structure optimization. None of the atoms in the adsorbed acetic acid, methanol, and water molecules were constrained in the optimization of the adsorption complexes. The calculations, which included structure optimization and single-point energies, employed the hybrid density functional B3LYP method with standard DZVP2 basis sets. All of the calculations were performed using the Gaussian03 program package.

3. Results and discussion

The propylsulfonic acid-functionalized SBA-15 materials used in the study were analyzed for their textural properties. The N_2 adsorption–desorption isotherms of the samples had type IV hysteresis loops with sharp adsorption and desorption curves, as seen

in Fig. 1, which were consistent with mesoporous materials tailored by nonionic templates [17,18]. The BET surface area of 620 m^2/g was also in the range reported in the literature for these types of mesoporous materials [15,17]. The sulfur content of the sulfonic acid-functionalized SBA-15 materials was determined to be 1.29 mmol/g by elemental analysis, which was consistent with the amount added during the synthesis. The carbon/sulfur molar ratio was 3.5, which was a little higher than the theoretical value of 3, indicating that the template was not completely removed by extraction with ethanol reflux. The number of accessible organosulfonic acid groups in the mesoporous silica was quantitatively determined to be 1.07 meq/g by acid–base titration in good agreement with the elemental analysis for the sulfur. As shown in Fig. 2, the TGA analysis of the sample further confirmed that the thiol groups had been successfully oxidized to sulfonic acid groups as demonstrated by the weight loss peak at about 723 K. The combined characterization results confirmed the successful incorporation of the organosulfonic acid groups into the surface of SBA-15 while maintaining the mesoporous structure of the support and the accessibility of the acidic sites.

An important goal of this study was to determine whether there was a mechanistic difference between a homogeneous catalyst and its supported analog. The homogeneous acid-catalyzed esterification reaction is known to follow second-order kinetics, which are first order with respect to each reactant. The calculation of kinetic parameters for heterogeneous acid catalysts can be complicated due to complex catalyst surface–adsorbate interactions. As is typically done, the reaction orders were determined by varying the concentration of one reactant while fixing that of the other at 2.0 M and measuring initial reaction rates at 323 K. Table 1 summarizes the measured initial rates. The concentration of both acetic acid and methanol had positive effects on the reaction rate with increasing reactant concentration. By using power law approximation fitting, the apparent reaction orders were determined to be 0.72 for methanol and 0.87 for acetic acid, with a correlation coefficient of 0.99–1.00. The results are somewhat different than the values reported by Goodwin et al. [4], which is possibly the result of different acid catalysts being employed.

Since the functional groups grafted on SBA-15 were propylsulfonic acid groups, propane sulfonic acid, which bears the same structure as the functional groups grafted on SBA-15, was examined for comparison. Fig. 3 compares the intrinsic per site activity (turnover number, TON) for acetic acid esterification over propane sulfonic acid and SO_3H-SBA-15. The insert in Fig. 3 shows the initial reaction rate (below 10% conversion of the limiting reagent) over the two catalysts, which demonstrated a higher per site reaction rate with propane sulfonic acid than with SO_3H-SBA-15, indicating a lower

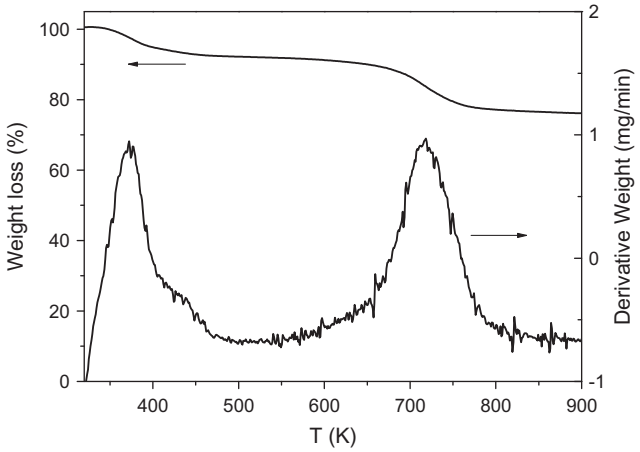

Fig. 2. TGA and DTG profiles of the propylsulfonic acid-functionalized SBA-15.

Table 1
Initial reaction rate data for the determination of apparent reaction orders of acetic acid and methanol in SO_3H-SBA-15-catalyzed esterification at 323 K.

$C_{A,0}$ (M)	$C_{M,0}$ (M)	r_0 (M/min) × 10^3
2	2	4.94
2	4	8.96
2	6	12.4
2	14	20.0
4	2	9.24
5	2	11.2
6	2	12.8

intrinsic activity for SO_3H-SBA-15 than propane sulfonic acid. As the organosulfonic acid sites within the mesoporous silica structure should be readily accessible to the reactants, the lower intrinsic activity shown by the heterogeneous catalyst may be due to the interaction of the strong Brønsted acidic sites with the silanol groups of the silica support, resulting in decreased activity for the organosulfonic acid group [19]. As discussed in our previous contribution [12], the amount of silanols on the propylsulfonic acid-functionalized SBA-15 was estimated to be significant relative to the number of organosulfonic acid groups. Alternatively, the more restricted conformation of the adsorbed intermediate onto the functionalized SBA-15 compared with those in the case of the homogeneous catalyst might result in the lower measured intrinsic activity of SO_3H-SBA-15. The discrepancy in intrinsic activity between heterogeneous catalysts and their homogeneous analogs has been reported

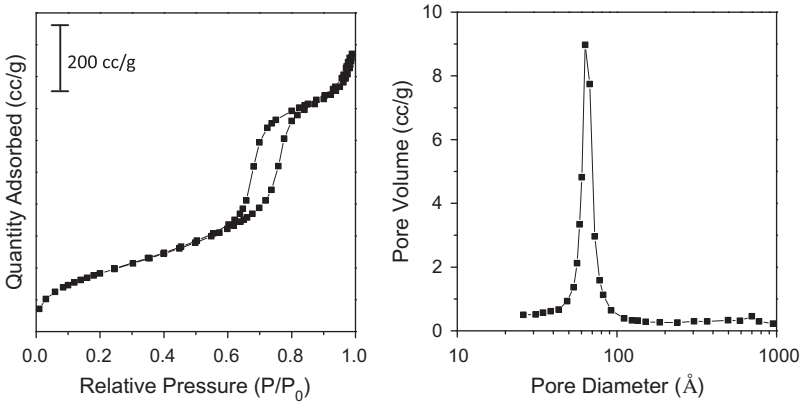

Fig. 1. N_2 adsorption–desorption isotherm and pore size distribution curve of for the SO_3H-SBA-15 material.

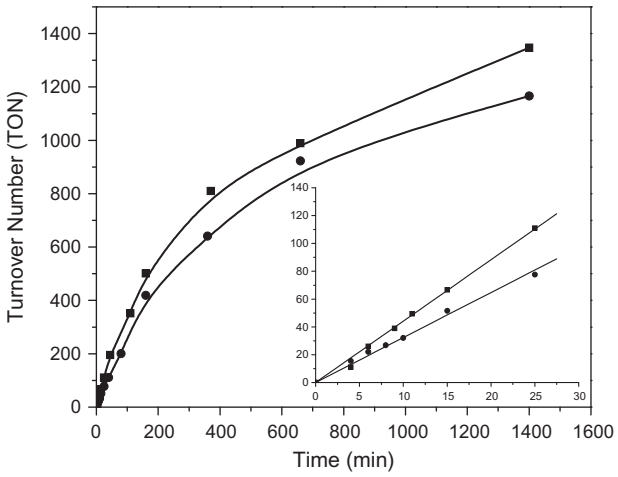

Fig. 3. Comparison of acetic acid esterification activity over propane sulfonic acid and SO_3H-SBA-15 ($C_{A,0}$ = 3 M, $C_{M,0}$ = 6 M, T = 323 K, 600 rpm); ■: propane sulfonic acid; ●: SO_3H-SBA-15.

for a number of reaction systems [20–22]. This difference has commonly been ascribed to both of the factors discussed above.

The apparent activation energies were determined for the two catalyst systems by performing reactions at 303, 313, 323, and 333 K. Since mass transfer limitation would not be an issue with the homogeneous propane sulfonic acid catalyst, comparison with the apparent activation energy for the heterogeneous SO_3H-SBA-15 provided further insight into whether mass transfer limitations play a role in the reactivity difference between the two catalyst systems. The results from the reaction temperature studies are shown in Fig. 4 with the apparent activation energies calculated, assuming a rate law that was first order in acetic acid concentration and zero order in methanol, since excess methanol was used. The apparent activation energy over propane sulfonic acid was found to be 36.4 kJ/mol, which was somewhat lower than that found for SO_3H-SBA-15 (42.6 kJ/mol). These results suggested that the SO_3H-SBA-15 catalyst was not limited by mass transfer or internal diffusion, which was not surprising given that the material had a median pore diameter of about 8 nm and the low reaction rates that were used.

To investigate the effect of reactant adsorption on reactivity, the heterogeneous catalyst was studied by premixing it with methanol, acetic acid or both methanol and acetic acid for 10 h at ambient temperature. After the reaction system reached the reaction temperature, the preheated remaining reactant was introduced. The conversion versus time data for these experiments are shown in Fig. 5. The result of the standard reaction protocol (heating the mixture of all the reactants to the desired temperature and then charging the catalyst) is also included in the figure for reference. The results showed that the reaction rate increased when premixing the catalyst with methanol or the mixture of methanol and acetic acid compared with the standard reaction protocol. The effect was particularly dramatic when the catalyst was premixed with both methanol and acetic acid. In contrast, the catalytic activity was dramatically decreased when the catalyst was premixed with acetic acid only. These results suggested that the esterification reaction over SO_3H-SBA-15 does not follow the single-site mechanism recently proposed for other solid acid catalysts [4,23,24]. The catalytic result that would be expected based on the above single-site mechanism would yield promotion of the catalytic reaction due to premixing with acetic acid. The results as shown in Fig. 5 suggested that the chemisorption of both acetic acid and methanol is essential for the catalytic reaction. It was also apparent from these results that the adsorption of acetic acid was stronger than that of methanol as the pre-adsorption of methanol did not inhibit the reaction as was the case with the pre-adsorption of acetic acid. This result was in disagreement with other reported results that proposed stronger adsorption of the alcohol than the acid [9,25].

In order to better compare with the analogous homogeneous acid catalyst, the same experiments were performed using propane sulfonic acid with the results shown in Fig. 6. As can be seen, the results were markedly different than that seen with SO_3H-SBA-15 as no difference in activity was observed with any of the premixing modes. This comparison suggested that the reaction mechanism over the homogeneous catalyst was different from that over the supported acid catalyst. Given the previous results in the literature, it appears the reaction with propane sulfonic acid followed the same mechanism as that with sulfuric acid and SAC-13, i.e., in which the acidic site on the catalyst promoted the protonation of the carbonyl oxygen on the carboxylic group in acetic acid, thereby activating nucleophilic attack by methanol to form a tetrahedral intermediate [2,4,24].

Additional experiments were performed to explore the kinetic pathways for the two catalytic systems. In these experiments, acetic acid esterification with methanol was performed over propane

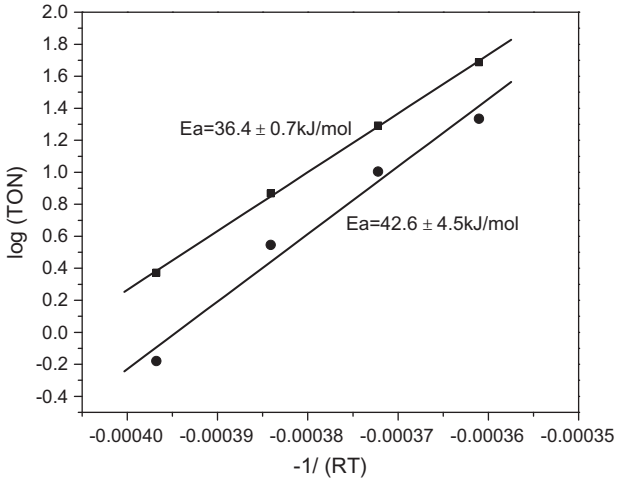

Fig. 4. Comparison of acetic acid esterification activity over propane sulfonic acid and SO_3H-SBA-15 at different temperatures ($C_{A,0}$ = 3 M, $C_{M,0}$ = 6 M); ■: propane sulfonic acid; ●: SO_3H-SBA-15.

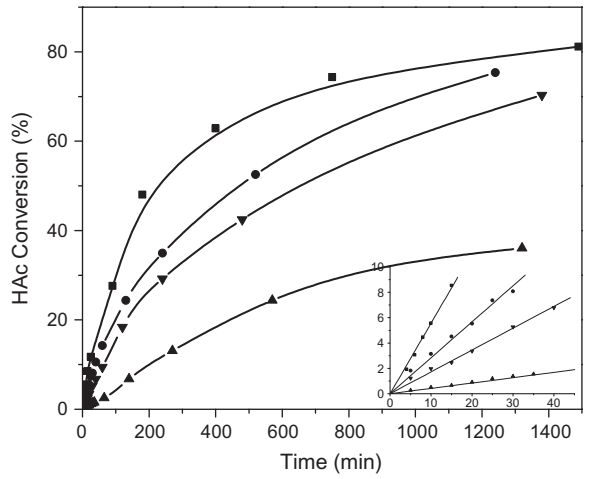

Fig. 5. Acetic acid conversion using different premixing of the reactants with the SO_3H-SBA-15 ($C_{A,0}$ = 3 M, $C_{M,0}$ = 6 M, T = 323 K, stirring speed = 600 rpm, inset: initial reaction period); ■: premixing with acetic acid and methanol; ●: premixing with methanol; ▼: no premixing; ▲: premixing with acetic acid.

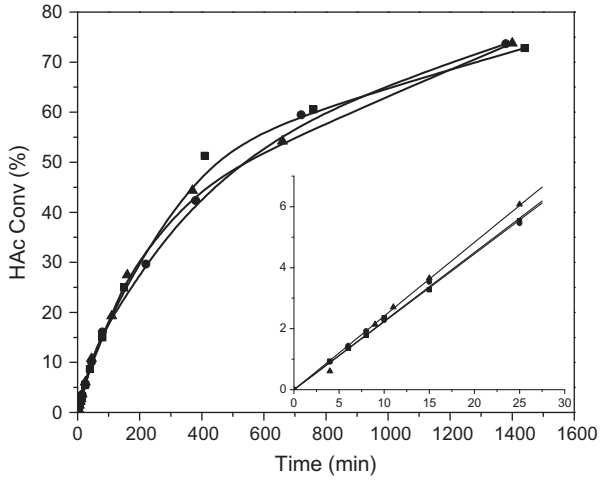

Fig. 6. Acetic acid conversion using different premixing of the reactants with propane sulfonic acid ($C_{A,0}$ = 3 M, $C_{M,0}$ = 6 M, T = 323 K, stirring speed = 600 rpm, inset: initial reaction period); ■: premixing with methanol; ●: premixing with acetic acid; ▲: no premixing.

sulfonic acid and SO_3H-SBA-15 with varying amounts of acidic sites. The experimental protocol used for these experiments was the same as that used by the Goodwin lab where the varying amounts of acidic sites were obtained by poisoning the same amount of catalyst with different amounts of pyridine [4]. The initial reaction rates were measured and then plotted as a function of the mmoles of acidic sites in the reaction system (Fig. 7). It is clear from these results that the initial reaction rates were linearly correlated with the number of acidic sites over propane sulfonic acid, while with SO_3H-SBA-15, the relationship between the initial reaction rates and the number of acidic sites was second order. This result further supported that the reaction with propane sulfonic acid followed a single-site mechanism, but that a dual-site mechanism applied for esterification with the SO_3H-SBA-15 catalyst.

In the kinetic behavior description of heterogeneously catalyzed esterification reactions, three different models have been applied: the quasi-homogeneous model (Q-H), the Eley–Rideal model (E–R) and the Langmuir–Hinselwood model (L–H) [26]. The Q-H model assumes complete swelling of the polymeric catalyst in contact with polar solvents, leading to improved access of the reactants to the active sites. This model is not applicable here since the catalytic material is not polymeric and does not swell in the solvent. The E–R and L–H mechanisms assume the catalytic surface reaction controls the overall process. The E–R model has been applied if in the rate-limiting step, surface reaction takes place between an adsorbed species and a non-adsorbed reactant from the bulk liquid phase. On the other hand, the L–H model is applicable whenever the rate-determining step is the surface reaction between adsorbed molecules.

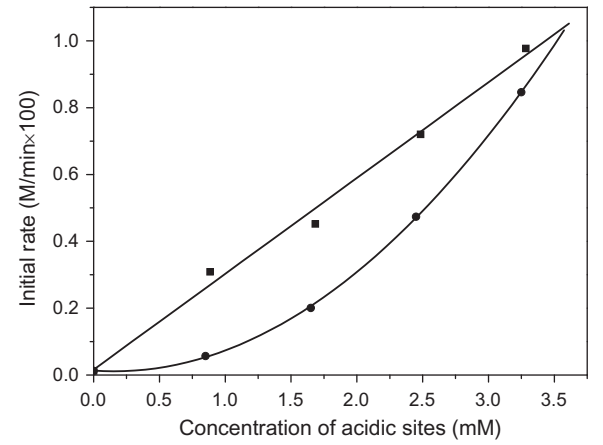

Fig. 7. Comparison of the initial esterification reaction rate as a function of the acid site concentrations over propylsulfonic acid-functionalized SBA-15 and propane sulfonic acid ($C_{A,0}$ = 3 M, $C_{M,0}$ = 6 M, 323 K, 600 rpm); ■: propane sulfonic acid; ●: SO_3H-SBA-15.

In determining a suitable model, one statistical approach is to evaluate the least sum of squares for the competing models. For the current work, reaction rates were calculated by the differential method as discussed by Cunill et al. [27] and Subramanian et al. [28]. Conversion data were fit as a function of time through a fifth-degree polynomial, whose slope allowed calculation of the reaction rate. In the case of the heterogeneously catalyzed esterification reaction, Eq. (1),

$$-r_A = \frac{n_{A,0}}{V}\left(\frac{dX_A}{dt}\right) \tag{1}$$

was applied, where $-r_A$ is the reaction rate of acetic acid, V is the volume of the reaction mixture, $n_{A,0}$ is the initial number of moles of acetic acid, X_A is the conversion of acetic acid, and t is the reaction time.

The nonideality of all the liquid components was taken into consideration by using their respective activities [9,25,26]. The UNIFAC group contribution method was employed for the estimation of activity coefficients [29]. The equilibrium constant was calculated from the component concentrations at equilibrium through Eq. (2),

$$K_{eq} = \left(\frac{\alpha_{MA}\alpha_W}{\alpha_A\alpha_M}\right)_{eq} = \left(\frac{x_{MA}x_W}{x_Ax_M}\right)_{eq}\left(\frac{\gamma_{MA}\gamma_W}{\gamma_A\gamma_M}\right)_{eq} = K_xK_\gamma \tag{2}$$

where K_{eq} is the reaction equilibrium constant, α is the component activity, x is the component mole fraction, and γ is the component activity coefficient. The subscripts A, M, MA, and W denote acetic acid, methanol, methyl acetate, and water, respectively.

The estimation of the parameters for the different models was performed by minimizing the sum of residual squares (SRS) between the experimental and calculated reaction rates (Eq. (3)) through the simplex algorithm [9,25].

$$\mathrm{SRS} = \sum_{samples}\left(r_{\exp} - r_{calc}\right)^2 \tag{3}$$

In Eq. (3), SRS is the minimum sum of residual squares resulting from the fitting procedure and r is the reaction rate. The subscripts *exp* and *calc* denote experimental and calculated values, respectively.

The improved Euler's numerical method was applied to integrate the equations describing the kinetic model with the previously determined parameters. Experimental results were then compared with those of the model prediction through the values of the mean relative deviation (MRD) between experimental and calculated conversions (Eq. (4)).

$$\mathrm{MRD} = \frac{1}{n}\left(\sum_{allsamples}\left|\frac{X_{A,cal} - X_{A,\exp}}{X_{A,\exp}}\right|\right) \times 100 \tag{4}$$

The rate equation resulting from the E–R model is expressed by Eq. (5),

$$r_A = \frac{A_f * \exp\left(\frac{-E_0}{RT}\right)\left(\alpha_A\alpha_M - \frac{\alpha_{MA}\alpha_W}{K_{eq}}\right)}{1 + K_A\alpha_A + K_M\alpha_M + K_{MA}\alpha_{MA} + K_W\alpha_W} \tag{5}$$

whereas the rate equation resulting from application of the L–H model is given by Eq. (6),

$$r_A = \frac{A_f * \exp\left(\frac{-E_0}{RT}\right)\left(\alpha_A\alpha_M - \frac{\alpha_{MA}\alpha_W}{K_{eq}}\right)}{\left(1 + K_A\alpha_A + K_M\alpha_M + K_{MA}\alpha_{MA} + K_W\alpha_W\right)^2} \quad (6)$$

In Eqs. (5) and (6), A_f is the Arrhenius pre-exponential factor for the forward reaction, E_0 is the apparent activation energy of the reaction, K_{eq} is the reaction equilibrium constant, R is the gas constant, and T is the reaction temperature. Parameters K_A, K_M, K_{MA} and K_W are the adsorption equilibrium constants for acetic acid, methanol, methyl acetate, and water, respectively.

The adsorption equilibrium constant for each component can be defined as the ratio of the adsorption rate constant to the desorption rate constant.

$$K_i = \frac{k_{a,i}}{k_{d,i}}, \quad i = A, M, MA, \text{ and } W \quad (7)$$

Table 2 compares the parameters for the E–R and L–H kinetic models found from fitting the experimental data. Also shown in the table are sum of residual squares resulting from the minimization process and the mean relative deviation between experimental and calculated acetic acid conversions. Both of the models fit the experimental data with very small errors. The apparent activation energies obtained for the two models were very similar and close to the value of 42.6 kJ/mol obtained experimentally. The value of the activation energy supported the supposition that the overall process was controlled by the surface reaction. Using the SRS and MRD values, the L–H model gave a better correlation between the experimental results and the model for the reaction system. Fig. 8 shows a comparison between the L–H model and the experimental kinetic data. Additionally, the acetic acid adsorption equilibrium constant was found to be higher than that of methanol, which was in agreement with the experimental observations described earlier.

To independently examine the adsorption of acetic acid and methanol molecules onto the acidic sites of tethered propylsulfonic acid groups and whether acetic acid could be expected to adsorb more strongly than methanol, the adsorption energies of acetic acid and methanol onto the acidic sites were calculated using the DFT method. Shown in Fig. 9 are the optimized structures found for acetic acid and methanol adsorbing on the model Si-tethered propylsulfonic acid complexes using the B3LYP/DZVP2 level. It is important to note that these structures only considered the interaction of adsorbing molecule with the simplified surface model as well as in the absence of the condensed phase. However, these structures could be expected to provide some relative energetic information concerning the adsorption of the reactant molecules. The adsorption energy of acetic acid for the structure in Fig. 9 was computed to be about 142 kJ/mol, while that of methanol was 59 kJ/mol. The results for this simplified system indicated that both acetic acid and methanol could adsorb on the propylsulfonic acid groups and that the adsorption of acetic acid was stronger than that of methanol. These results were in complete qualitative agreement with adsorption behavior found from the experimental and kinetic modeling results. The adsorption energy of a water molecule on the propylsulfonic acid group was calculated to be about 57 kJ/mol, which was almost the same as that of methanol. Therefore, acetic acid, methanol, and water all would be expected to adsorb competitively with methanol and water having similar

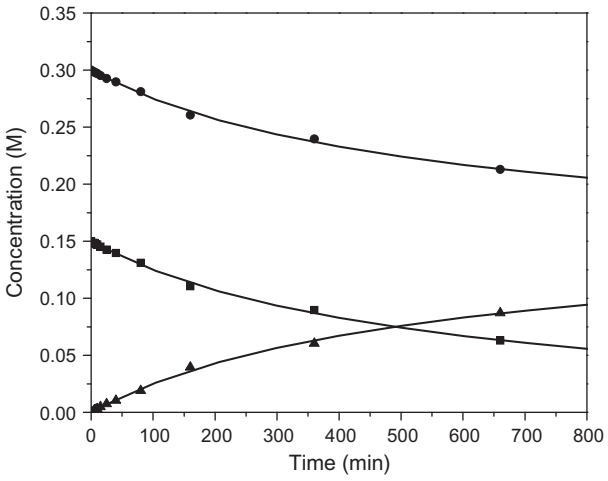

Fig. 8. Comparison between the experimental and L–H model calculated concentration profiles (feed mole ratio alcohol to acid 2:1, T = 323 K; stirring speed = 600 rpm); ■: acetic acid; ●: methanol; ▲: methyl acetate; —: L–H model.

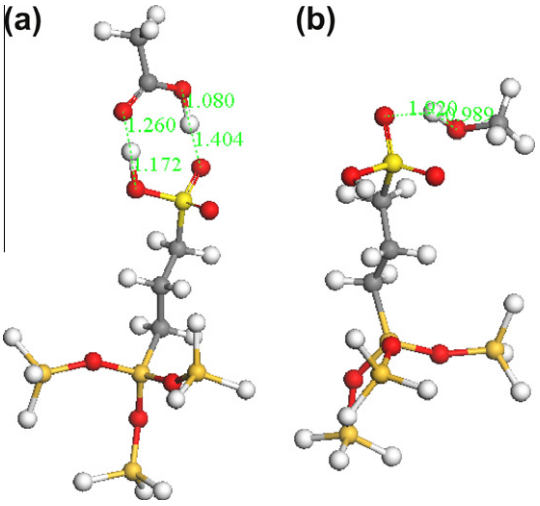

Fig. 9. Geometries of acetic acid (a) and methanol (b) adsorbed on SO_3H-SBA-15 as optimized by B3LYP/DZVP2.

adsorption energies, which was consistent with the L–H model that was derived from the experimental data.

The experimental and modeling results supported that esterification of acetic acid with methanol over propylsulfonic acid-functionalized SBA-15 followed a dual-site mechanism in which an adsorbed and protonated acetic acid molecule reacts with an adsorbed and non-protonated methanol molecule (Scheme 1). This result differed from some previous reports in which a single-site mechanism was found for heterogeneous acid catalysts [4,23,24]. In the single-site mechanism, a non-adsorbed methanol molecule reacts with an adsorbed acetic acid molecule, while both reactant molecules are required to be adsorbed in the dual-site mechanism. The adsorption of methanol molecules over acidic catalysts has been reported in the literature for the esterification reaction and

Table 2
Comparison of E–R and L–H model parameters found from fitting the experimental data.

Model	A_f (mol L^{-1} min^{-1})	E_0 (kJ/mol)	K_A	K_M	K_{MA}	K_W	SRS	MRD (%)
E–R	1.210×10^6	45.61	5.11	0	0	3.41	1.42×10^{-8}	0.896
L–H	1.481×10^6	42.32	5.15	1.64	0.15	3.23	3.62×10^{-9}	0.678

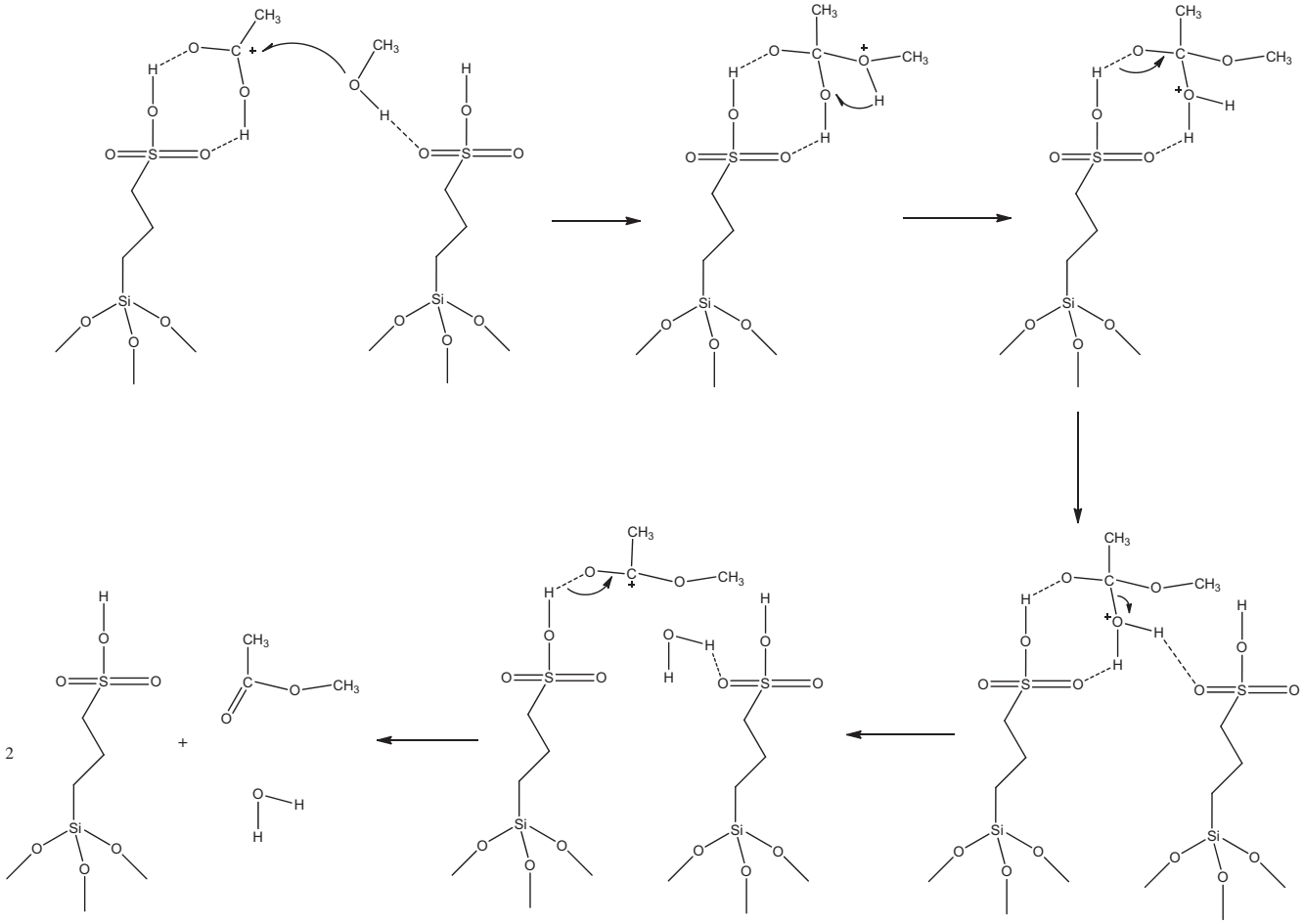

Scheme 1. Possible reaction mechanism for the acetic acid esterification with methanol over propylsulfonic acid-functionalized SBA-15.

other acid-catalyzed reactions [25,30,31]. The reaction mechanism appears to depend on the type of heterogeneous catalyst since the methodology used in this study was similar to that used by Liu et al., but with a different catalyst [4]. The active sites on the catalysts were similar, but the supports were different, which could modify the adsorption of methanol.

4. Conclusion

This work focused on the investigation of the reaction mechanism of acetic acid esterification with methanol over a propylsulfonic acid-functionalized SBA-15 catalyst, which was prepared using the co-condensation method. To investigate the difference between heterogeneous and homogeneous catalyzed esterification, a homogeneous catalyst, propane sulfonic acid, was used for the reaction as it had the same structure as the functional groups grafted on the silica. For the heterogeneous catalyzed system, the apparent reaction orders were determined to be 0.72 for methanol and 0.87 for acetic acid, with a correlation coefficient of 0.99–1.00. Pre-adsorption experiments showed that pre-adsorption of acetic acid hindered the reaction rate, while pre-adsorption of methanol or acetic acid with methanol increased the reaction rate, which indicated that acetic acid adsorbs more strongly than methanol over the heterogeneous acid catalyst. However, it was found that the esterification of acetic acid with methanol over the functionalized SBA-15 catalyst followed a L–H reaction mechanism, which required adsorption of both acetic acid and methanol. While over the homogeneous catalyst, esterification followed the E–R mechanism. The kinetic data for the heterogeneous catalyst system were successfully fit using a L–H model with the surface reaction as the rate-limiting step.

Acknowledgment

This work was supported by ConocoPhillips Company. The first author acknowledges the Dalian Institute of Chemical Physics, Chinese Academy of Sciences, for use of their computational facility.

Appendix A. Supplementary material

Supplementary data associated with this article can be found, in the online version, at doi:10.1016/j.jcat.2011.01.008.

References

[1] G.D. Yadav, P.H. Mehta, Ind. Eng. Chem. Res. 33 (1994) 2198–2208.
[2] R. Ronnback, T. Salmi, A. Vuori, H. Haario, J. Lehtonen, A. Sundqvist, E. Tirronen, Chem. Eng. Sci. 52 (1997) 3369–3381.
[3] R. Koster, B. van der Linden, E. Poels, A. Bliek, J. Catal. 204 (2001) 333–338.
[4] Y.J. Liu, E. Lotero, J.G. Goodwin, J. Catal. 242 (2006) 278–286.
[5] S.R. Kirumakki, N. Nagaraju, S. Narayanan, Appl. Catal. A 273 (2004) 1–9.
[6] K. Suwannakarn, E. Lotero, J.G. Goodwin, Ind. Eng. Chem. Res. 46 (2007) 7050–7056.
[7] T.A. Nijhuis, A.E.W. Beers, F. Kapteijn, J.A. Moulijn, Chem. Eng. Sci. 57 (2002) 1627–1632.
[8] B.R. Jermy, A. Pandurangan, Appl. Catal. A 288 (2005) 25–33.
[9] H.T.R. Teo, B. Saha, J. Catal. 228 (2004) 174–182.
[10] M.J. Lee, H.T. Wu, H.M. Lin, Ind. Eng. Chem. Res. 39 (2000) 4094–4099.
[11] W.L. Chu, X.G. Yang, X.K. Ye, Y. Wu, Appl. Catal. A 145 (1996) 125–140.
[12] S. Miao, B.H. Shanks, Appl. Catal. A 359 (2009) 113–120.

[13] F.H. Mahfud, I. Melian-Cabrera, R. Manurung, H.J. Heeres, IChemE B, Process Saf. Environ. Protect. 85 (2007) 466–472.
[14] D. Margolese, J.A. Melero, S.C. Christiansen, B.F. Chmelka, G.D. Stucky, Chem. Mater. 12 (2000) 2448–2459.
[15] I.K. Mbaraka, D.R. Radu, V.S.Y. Lin, B.H. Shanks, J. Catal. 219 (2003) 329–336.
[16] W.M. Van Rhijn, D.E. De Vos, B.F. Sels, W.D. Bossaert, P.A. Jacobs, Chem. Commun. (1998) 317–318.
[17] I.K. Mbaraka, B.H. Shanks, J. Catal. 229 (2005) 365–373.
[18] W.Z. Zhang, B. Glomski, T.R. Pauly, T.J. Pinnavaia, Chem. Commun. (1999) 1803–1804.
[19] P. Botella, A. Corma, J.M. Lopez-Nieto, J. Catal. 185 (1999) 371–377.
[20] S. Xiang, Y.L. Zhang, Q. Xin, C. Li, Angew. Chem. Int. Ed. 41 (2002) 821–824.
[21] S. Xiang, Y.L. Zhang, Q. Xin, C. Li, Chem. Commun. (2002) 2696–2697.
[22] A. Choplin, F. Quignard, Coord. Chem. Rev. 178–180 (1998) 1679–1702.
[23] Y.J. Liu, E. Lotero, J.G. Goodwin, J. Mol. Catal. A 245 (2006) 132–140.
[24] E. Lotero, Y.J. Liu, D.E. López, K. Suwannakarn, D.A. Bruce, J.G. Goodwin, Ind. Eng. Chem. Res. 44 (2005) 5353–5363.
[25] M.T. Sanz, R. Murga, S. Beltran, J.L. Cabezas, J. Coca, Ind. Eng. Chem. Res. 41 (2002) 512–517.
[26] L.K. Rihko, A.O.I. Krause, Ind. Eng. Chem. Res. 34 (1995) 1172–1180.
[27] F. Cunill, M. Iborra, C. Fité, J. Tejero, J.F. Izquierdo, Ind. Eng. Chem. Res. 39 (2000) 1235–1241.
[28] P.M. Subramanian, S.K. Chatterjee, M.C. Bhatia, J. Chem. Technol. Biotechnol. 39 (1987) 215–218.
[29] B.E. Poling, J.M. Prausnitz, J.P. O'Connell, The Properties of Gases and Liquids, fifth ed., 2000.
[30] M. Xu, J.H. Lunsford, D.W. Goodman, A. Bhattacharyya, Appl. Catal. A 149 (1997) 289–301.
[31] J. Limtrakul, Chem. Phys. 193 (1995) 79–87.